

# Conservative cosmology: combining data with allowance for unknown systematics

José Luis Bernal<sup>a,b</sup> John A. Peacock<sup>c</sup>

<sup>a</sup>ICC, University of Barcelona, IEEC-UB, Martí i Franquès, 1, E08028 Barcelona, Spain

<sup>b</sup>Dept. de Física Quàntica i Astrofísica, Universitat de Barcelona, Martí i Franquès 1, E08028 Barcelona, Spain

<sup>c</sup>Institute for Astronomy, University of Edinburgh, Royal Observatory, Blackford Hill, Edinburgh, EH9 3HJ, UK

E-mail: [joseluis.bernal@icc.ub.edu](mailto:joseluis.bernal@icc.ub.edu), [jap@roe.ac.uk](mailto:jap@roe.ac.uk)

**Abstract.** When combining data sets to perform parameter inference, the results will be unreliable if there are unknown systematics in data or models. Here we introduce a flexible methodology, **BACCUS**: Bayesian Conservative Constraints and Unknown Systematics, which deals in a conservative way with the problem of data combination, for any degree of tension between experiments. We introduce parameters that describe a bias in each model parameter for each class of experiments. A conservative posterior for the model parameters is then obtained by marginalization both over these unknown shifts and over the width of their prior. We contrast this approach with an existing method in which each individual likelihood is scaled, comparing the performance of each approach and their combination in application to some idealized models. Using only these rescaling is not a suitable approach for the current observational situation, in which internal null tests of the errors are passed, and yet different experiments prefer models that are in poor agreement. The possible existence of large shift systematics cannot be constrained with a small number of data sets, leading to extended tails on the conservative posterior distributions. We illustrate our method with the case of the  $H_0$  tension between results from the cosmic distance ladder and physical measurements that rely on the standard cosmological model.

---

## Contents

<b>1</b>	<b>Introduction</b>	<b>1</b>
<b>2</b>	<b>Overview of assumptions and methodology</b>	<b>2</b>
<b>3</b>	<b>Application to illustrative examples</b>	<b>4</b>
3.1	Shift parameters in the one-parameter Gaussian case	4
3.2	Contrasting shift and rescaling parameters	7
3.3	Examples with multiple parameters	7
<b>4</b>	<b>Applications to cosmology: <math>H_0</math></b>	<b>9</b>
4.1	Data and modelling	9
4.2	Results	11
<b>5</b>	<b>Summary and discussion</b>	<b>14</b>

---

## 1 Introduction

For two decades or more, the standard  $\Lambda$ -Cold Dark Matter ( $\Lambda$ CDM) cosmological model has succeeded astonishingly well in matching new astronomical observations, and its parameters are precisely constrained (e.g. [1–3]). However, more recent work has persistently revealed tensions between high and low redshift observables. In the case of the Hubble constant,  $H_0$ , the best direct measurement using cepheids and supernovae type Ia [4] is in  $3.4\sigma$  tension with the value inferred assuming  $\Lambda$ CDM using Planck observations [1]. Planck and weak lensing surveys both measure the normalization of density fluctuations via the combination  $\Omega_m^{0.5}\sigma_8$ , and their estimates were claimed to be in  $2.3\sigma$  tension by the KiDS collaboration [5] – although recent results from DES are less discrepant [6]. These inconsistencies are not currently definitive (e.g. [7]), but they raise the concern that something could be missing in our current cosmological understanding. It could be that the  $\Lambda$ CDM model needs extending, but it could also be that the existing experimental results suffer from unaccounted-for systematics or underestimated errors.

When inconsistent data are combined naively, it is well understood that the results risk being inaccurate and that formal errors may be unrealistically small. For this reason, much emphasis is placed on tests that can be used to assess the consistency between two data sets (e.g. [8–10]). We refer the interested reader to [11, 12] for more methodologies but also for a comprehensive comparison between different measures of discordance. Another approach is the posterior predictive distribution, which is the sampling distribution for new data given existing data and a model, as used in e.g., [13]. However, these methods are not really helpful in cases of mild tension, where a subjective binary decision is required as to whether or not a genuine inconsistency exists.

Unknown systematics can be modelled as the combination of two distinct types. Type 1 systematics affect the random scatter in the measurements (and therefore the size of the errors in a parameterised model), but do not change the maximum-posterior values for the parameters of the model. In contrast, type 2 systematics offset the best-fitting parameters without altering the random errors; they are completely equivalent to shifts in the parameters of the model without modifying the shape of the posterior of each parameter. While the former are commonly detectable through internal evidence, the latter are more dangerous and they can only reveal themselves when independent experiments are compared. Much of our discussion will focus on this class of systematic. With a detailed understanding of a given experiment, one could do better than this simple classification; but here we are trying to capture ‘unknown unknowns’ that have evaded the existing modelling of systematics, and so the focus must be on the general character of these additional systematics.

Taking all this into account, there is a need for a general conservative approach to the combination of data. This method should allow for possible unknown systematics of both kinds and it should permit

the combination of data sets in tension with an agnostic perspective. Such a method will inevitably yield uncertainties in the inferred parameters that are larger than in the conventional approach, but having realistic uncertainties is important if we are to establish any credible claims for the detection of new physics.

The desired method can be built using a hierarchical approach. Hierarchical schemes have been used widely in cosmology, e.g. to model in more detail the dependence of the parameters on each measurement in the case of  $H_0$  and the cosmic distance ladder [14], or the cosmic shear power spectrum [15]. While the extra parameters often model physical quantities, our application simply requires empirical nuisance parameters. The introduction of extra parameters to deal with data combination was first introduced in the pioneering discussion of [16]. A more general formulation was provided by [17] and refined in [18] (H02 hereinafter). This work assigns a free weight to each data set, rescaling the logarithm of each individual likelihood (which is equivalent to rescaling the errors of each experiment if the likelihood is Gaussian), in order to achieve an overall reduced  $\chi^2$  close to unity. The H02 method yields meaningful constraints when combining data sets affected by type 1 errors, and it detects the presence of the errors by comparing the relative evidences of the conventional combination of data and their approach. However, this method is not appropriate for obtaining reliable constraints in the presence of type 2 systematics, where we might find several experiments that all have reduced  $\chi^2$  values of unity, but with respect to different best-fitting models. H02 do not make our distinction between different types of systematics, but in fact they do show an example where one of the data sets has a systematic type 2 shift (see Figures 3 & 4 of H02). Although their method does detect the presence of the systematic, we do not feel that it gives a satisfactory posterior in this case, for reasons discussed below in section 3.2.

Here we present a method called **BACCUS**<sup>1</sup>, **B**Ayesian **C**onservative **C**onstraints and **U**nknown **S**ystematics, which is designed to deal with systematics of both types. Rather than weighting each data set, the optimal way to account for type 2 systematics is to consider the possibility that the parameters preferred by each experiment are offset from the true values. Therefore, extra parameters shift the model parameters when computing each individual likelihood, and marginalized posteriors of the model parameters will account for the possible existence of systematics in a consistent way. Moreover, studying the marginalized posteriors of these new parameters can reveal which experiments are most strongly affected by systematics.

This paper is structured as follows. In Section 2, we introduce our method and its key underlying assumptions. In Section 3, we consider a number of illustrative examples of data sets constructed to exhibit both concordance and discordance, contrasting the results from our approach with those of H02. We then apply our method to a genuine cosmological problem, the tension in  $H_0$ , in Section 4. Finally, a summary and some general discussion of the results can be found in Section 5. We use the Monte Carlo sampler **emcee** [19] in all the cases where Monte Carlo Markov Chains are employed.

## 2 Overview of assumptions and methodology

We begin by listing the key assumptions that underlie our statistical approach to the problem of unknown systematics. Firstly, we will group all codependent experiments in different *classes*, and consider each of them independent from the others. For example, observations performed with the same telescope or analyzed employing the same pipeline or model assumptions will be considered in the same class, since all the really dangerous systematics would be in common. Then, our fundamental assumption regarding systematics will be that a experiment belonging to each of these classes is equally likely to commit an error of a given magnitude, and that these errors will be randomly and independently drawn from some prior distribution. Attempts have been made to allow for dependence between data sets when introducing scaling parameters as in H02 (see [20]). We believe that a similar extension of our approach should be possible, but we will not pursue this complication here.

With this preamble, we can now present the formalism to be used. Consider a model  $M$ , parameterised by a set of model parameters,  $\theta$  (we will refer to  $M(\theta)$  as  $\theta$  for simplicity), which are

---

<sup>1</sup>A python package implementing is publicly available in <https://github.com/jl-bernal/BACCUS>.

to be constrained by several data sets,  $\mathbf{D}$ . The corresponding posterior,  $\mathcal{P}(\boldsymbol{\theta}|\mathbf{D})$ , and the likelihood,  $\mathcal{P}(\mathbf{D}|\boldsymbol{\theta})$ , are related by the Bayes theorem:

$$\mathcal{P}(\boldsymbol{\theta}|\mathbf{D}) = \frac{\mathcal{P}(\boldsymbol{\theta}) \mathcal{P}(\mathbf{D}|\boldsymbol{\theta})}{\mathcal{P}(\mathbf{D})}, \quad (2.1)$$

where  $\mathcal{P}(\boldsymbol{\theta})$  is the prior. We will consider flat priors in what follows and concentrate on the likelihood, unless otherwise stated. For parameter inference, we can drop the normalization without loss of generality.

We can account for the presence of the two types of systematics in the data by introducing new parameters. For type 2 systematics, the best fit values of the parameters for each experiment,  $\tilde{\boldsymbol{\theta}}_i$ , may be offset from the true value by some amount. We introduce a shift parameter,  $\Delta_{\theta_j}^i$ , for each parameter  $\theta_j$  and class  $i$  of experiments. For type 1 systematics, we follow H02 and introduce a rescaling parameter  $\alpha_i$  which weights the logarithm of the likelihood of each class of experiments; if the likelihood is Gaussian, this is equivalent to rescaling each individual  $\chi^2$  and therefore the covariance. Considering  $n_i$  data points for the class of experiments  $i$ , the likelihood is now:

$$\mathcal{P}(\boldsymbol{\theta}, \boldsymbol{\alpha}, \{\boldsymbol{\Delta}_{\theta}\}|\mathbf{D}) \propto \prod_i \alpha_i^{n_i/2} \exp \left[ -\frac{\alpha_i}{2} \left( \chi_{\text{bf},i}^2 + \Delta \chi_i^2(\boldsymbol{\theta} + \boldsymbol{\Delta}_{\theta}^i - \tilde{\boldsymbol{\theta}}_i) \right) \right], \quad (2.2)$$

where  $\chi_{\text{bf}}^2$  is the minimum  $\chi^2$ , corresponding to the best-fit value of  $\boldsymbol{\theta}$ ,  $\tilde{\boldsymbol{\theta}}$ . Here, we use the notation  $\{\boldsymbol{\Delta}_{\theta}\}$  to indicate the vector of shift parameters for each parameter of the model. There is a different vector of this sort for every class of experiments, indexed by  $i$ .

For rescaling parameters, H02 argue that the prior should be taken as:

$$\mathcal{P}(\alpha_i) = \exp[-\alpha_i] \quad (2.3)$$

so that the mean value of  $\alpha_i$  over the prior is unity, i.e. experiments estimate the size of their random errors correctly on average. One might quarrel with this and suspect that underestimation of errors could be more common, but we will retain the H02 choice; this does not affect the results significantly. In realistic cases where the number of degrees of freedom is large and null tests are passed so that  $\chi_{\text{bf},i}^2 \simeq n$ , the scope for rescaling the errors will be small and  $\alpha_i$  will be forced to be close to unity. For the prior on shift parameters, we choose a zero-mean Gaussian with a different unknown standard deviation determined by  $\sigma_{\theta_j}$ , corresponding to each parameter  $\theta_j$  and common to all classes of experiments. Furthermore, it is easy to imagine systematics that might shift several parameters in a correlated way, so that the prior on the shifts should involve a full covariance matrix,  $\boldsymbol{\Sigma}_{\Delta}$ , containing the variances,  $\sigma_{\theta_j}^2$ , in the diagonal and off-diagonal terms obtained with the correlations  $\rho_{j_1, j_2}$  for each pair of shifts ( $\Sigma_{j_1, j_2} = \rho_{j_1, j_2} \sigma_{\theta_{j_1}} \sigma_{\theta_{j_2}}$ ). Thus the assumed prior on the shifts is:

$$\mathcal{P}(\{\boldsymbol{\Delta}_{\theta}\}|\boldsymbol{\sigma}_{\theta}, \boldsymbol{\rho}) \propto \prod_i^N |\boldsymbol{\Sigma}_{\Delta}|^{-1/2} \exp \left[ -\frac{1}{2} \boldsymbol{\Delta}_{\theta}^{i\text{T}} \boldsymbol{\Sigma}_{\Delta}^{-1} \boldsymbol{\Delta}_{\theta}^i \right]. \quad (2.4)$$

We now need to specify the hyperpriors for the covariance matrix of the shifts,  $\boldsymbol{\Sigma}_{\Delta}$ . Our philosophy here is to seek an uninformative hyperprior: it is safer to allow the data to limit the degree of possible systematic shifts, rather than imposing a constraining prior that risks forcing the shifts to be unrealistically small.

Different options of priors for covariance matrices are discussed by e.g. [21]. In order to ensure independence among variances and correlations, we use a separation strategy, applying different priors to variances and correlations (e.g. [22]). A covariance matrix can be expressed as  $\boldsymbol{\Sigma} = \mathbf{S}\mathbf{R}\mathbf{S}$ , with  $\mathbf{S}$  being a diagonal matrix with  $S_{jj} = \sigma_{\theta_j}$  and  $\mathbf{R}$ , the correlation matrix, with  $R_{ii} = 1$  and  $R_{ij} = \rho_{ij}$ . As hyperprior for each of the covariances we choose a lognormal distribution ( $\log \sigma = N(b, \xi)$ , where  $N(b, \xi)$  is a Gaussian distribution in  $\log \sigma$  with mean value  $b$  and variance  $\xi$ ). In the case of the correlation matrix, we use the LKJ distribution [23] as hyperprior, which depends only on the parameter  $\eta$ : for  $\eta = 1$ , it is an uniform prior over all correlation matrices of a given order; for  $\eta > 1$ , lower absolute correlations are favoured (and vice versa for  $\eta < 1$ ). The parameters  $b$ ,  $\xi$  and  $\eta$  can be

chosen to suit the needs of the specific problem. We prefer to be as agnostic as possible, so we will choose  $\eta = 1$  and  $b$  and  $\xi$  such as the hyperprior of each covariance is broad enough to not to force the shifts to be small.

The final posterior can be marginalized over all added parameters, leaving the conservative distribution of the model parameters  $\theta$ , that is the main aim of this work. This immediately provides a striking insight: a single experiment gives no information whatsoever. It is only when we have several experiments that the possibility of large  $\sigma_\theta$  starts to become constrained (so that the  $\{\Delta_\theta\}$  cannot be too large). In the case of consistent data, as the shifts are drawn from a Gaussian distribution, only small shifts are favoured (as the individual likelihoods would not overlap otherwise). If, on the other hand, only two data sets are available and there is a tension between them regarding some parameter  $\theta_j$ , the prior width  $\sigma_{\theta_j}$  could be of the order of such tension, but much larger values will be disfavoured.

However, an alternative would be to obtain the marginalized posteriors of  $\{\Delta_\theta\}$ . This tells us the likely range of shifts that each data set needs for each parameter, so that unusually discrepant experiments can be identified by the system. As we will see in examples below, this automatically results in their contribution to the final posterior being downweighted. If one class of experiments has shifts that are far beyond all others, this might give an objective reason to repeat the analysis without it, but generally we prefer not to take this approach: judging whether an offset is significant enough to merit exclusion is a somewhat arbitrary decision, and is complicated in a multidimensional parameter space. Our formalism automatically downweights data sets as their degree of inconsistency grows, and this seems sufficient.

### 3 Application to illustrative examples

#### 3.1 Shift parameters in the one-parameter Gaussian case

In order to exhibit all the features of our method more clearly, we first apply the formalism to the simple model in which there is only one parameter ( $\theta = a$ ) and the probability density functions (PDFs) of  $a$  for the  $N$  individual experiments are Gaussian. In this case, we can rewrite Equation 2.2 as:

$$\mathcal{P}(a, \alpha, \Delta_a, \sigma_a | \mathbf{D}) \propto \prod_i^N \alpha_i^{n_i/2} \exp \left[ -\frac{1}{2} \alpha_i (\chi_{i,\text{bf}}^2 + \Delta \chi_i^2 (a + \Delta_a^i)) \right]. \quad (3.1)$$

We apply the prior for rescaling parameters (Equation 2.3) and marginalize over each  $\alpha_i$  to obtain the marginalized posterior for a single class of experiments:

$$\mathcal{P}_i(a, \Delta_a^i, \sigma_a | D_i) \propto (\Delta \chi_i^2 (a + \Delta_a^i) + 2)^{-(n_i/2+1)}. \quad (3.2)$$

For large  $n_i$ ,  $\chi_i^2 + 2 \simeq \chi_i^2$ , and the right hand side of Equation 3.2 is proportional to  $\exp[-(\Delta \chi_i^2/2)(n_i/\chi_{i,\text{bf}}^2)]$ , which in effect instructs us to rescale parameter uncertainties according to  $(\chi_{\nu,i}^2)^{1/2}$ , where  $\chi_{\nu,i}^2$  is the reduced  $\chi_i^2$  for the class of experiments  $i$ . But it can be assumed that experiments will pursue internal null tests to the point where  $\chi_\nu^2 \simeq 1$ ; thus in practice rescaling parameters can do little to erase tensions.

Assuming hereafter that experimenters will achieve  $\chi_\nu = 1$  exactly, we can now focus on the novel feature of our approach, which is the introduction of shift parameters. Then, the posterior can be written as

$$\mathcal{P}(a, \Delta_a, \sigma_a | \mathbf{D}) \propto \prod_i^N \sigma_a^{-1} \exp \left[ -\frac{1}{2} \sum_{k=1}^{n_i} \left( \frac{(y_i^k(a + \Delta_a^i) - D_i^k)^2}{\sigma_i^{k2}} \right) + \frac{\Delta_a^i 2}{2\sigma_a^2} \right], \quad (3.3)$$

where  $y_i^k(x)$  is the theoretical prediction to fit to the measurement  $D_i^k$  of the class of experiments  $i$ , with error  $\sigma_i^k$ . Note that the width of the prior for the shifts,  $\sigma_a$ , is the same for all data sets, by

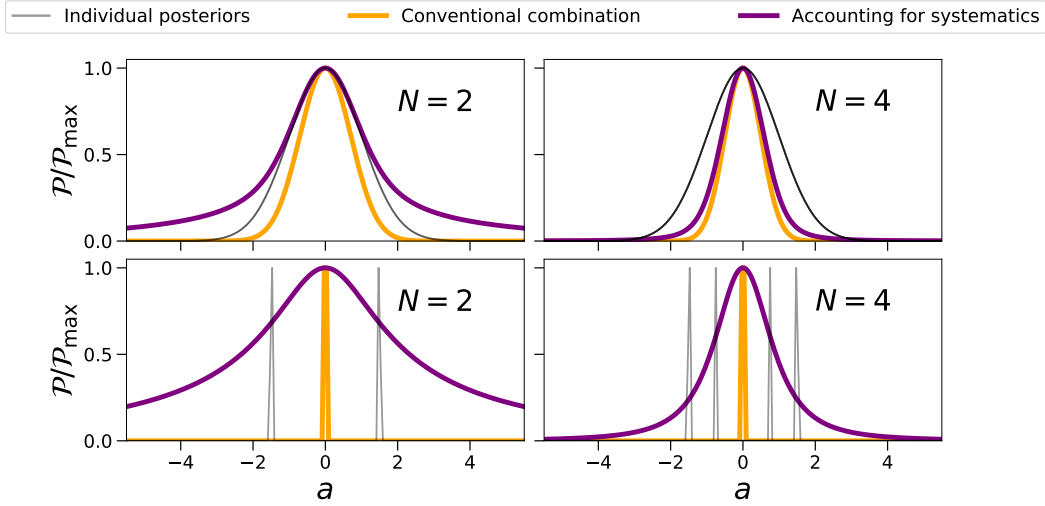


**Figure 1.** Comparison of the results obtained using shift parameters and the conventional approach to combining data sets in a model with only one parameter,  $a$ , and  $N$  data sets whose individual posteriors are Gaussians. We show individual posteriors in black, the posteriors obtained with the conventional approach in orange and the posterior obtained with our approach, in purple. The dependence of the posterior on the number of data sets for the exactly consistent case is shown in the top panels, while strongly inconsistent cases are shown in the bottom panels.

assumption. Marginalizing over the shifts, then the posterior of each class of experiments is:

$$\mathcal{P}_i(a, \sigma_a | \mathbf{D}) \propto \prod_{k=1}^{n_i} (\sigma_i^{k2} + \sigma_a^2)^{-1/2} \exp \left[ -\frac{1}{2} \frac{(y_i^k(a) - D_i^k)^2}{(\sigma_i^{k2} + \sigma_a^2)^2} \right]. \quad (3.4)$$

Therefore, our method applied to a model with only one parameter and Gaussian likelihoods reduces to the convolution of the original posteriors with a Gaussian of width  $\sigma_a$ .

Finally, we need to marginalize over  $\sigma_a$ . Consider for example a hyperprior wide enough to be approximated as uniform in  $\sigma_a$ , and suppose that all the  $N$  data sets agree on  $\tilde{a}_i = 0$  and all the errors,  $\sigma_i^k = \sigma_i$ , are identical. Then we can derive the marginalized posterior in the limit of small and large  $a$ :

$$\mathcal{P}(a | \mathbf{D}) \propto \begin{cases} 1 - \exp \left[ -\frac{(N-1)a^2}{2\sigma_i^2} \right], & \text{for } a \ll 1 \\ a^{1-N}, & \text{for } a \gg 1 \end{cases} \quad (3.5)$$

For values of  $a$  close to  $\tilde{a}_i$  the posterior presents a Gaussian core, whose width is  $\sigma_i/\sqrt{N-1}$ , in contrast with the conventional  $\sigma_i/\sqrt{N}$  from averaging compatible data. For values of  $a$  very far from  $\tilde{a}_i$ , the posterior has non-Gaussian power-law tails. For  $N = 2$  these are so severe that the distribution cannot be normalized, so in fact three measurements is the minimum requirement to obtain well-defined posteriors. As will be discussed in Section 5, one can avoid such divergence by choosing harder priors on  $\Delta_a^i$  or  $\sigma_a$ , but we prefer to be as agnostic as possible. Nonetheless, these ‘fat tails’ on the posterior are less of an issue as  $N$  increases. These two aspects of compatible data can be appreciated in the top panels of Figure 1. The message here is relatively optimistic: provided we have a number of compatible data sets, the conservative posterior is not greatly different from the conventional one.

Alternatively, we can consider an example of strongly incompatible data. Let the  $N$  data sets have negligible  $\sigma_i$  and suppose the corresponding  $\tilde{a}_i$  are disposed symmetrically about  $a = 0$  with spacing  $\epsilon$ , e.g.  $\tilde{a} = (-\epsilon, 0, +\epsilon)$  for  $N = 3$ . This gives a marginalized posterior that depends on  $N$ . For example, the tails follow a power law:  $\mathcal{P}(a | \mathbf{D}) \propto (1 + 4a^2/\epsilon^2)^{-1/2}$  for  $N = 2$ ,  $\mathcal{P}(a | \mathbf{D}) \propto (1 + 3a^2/2\epsilon^2)^{-1}$  for

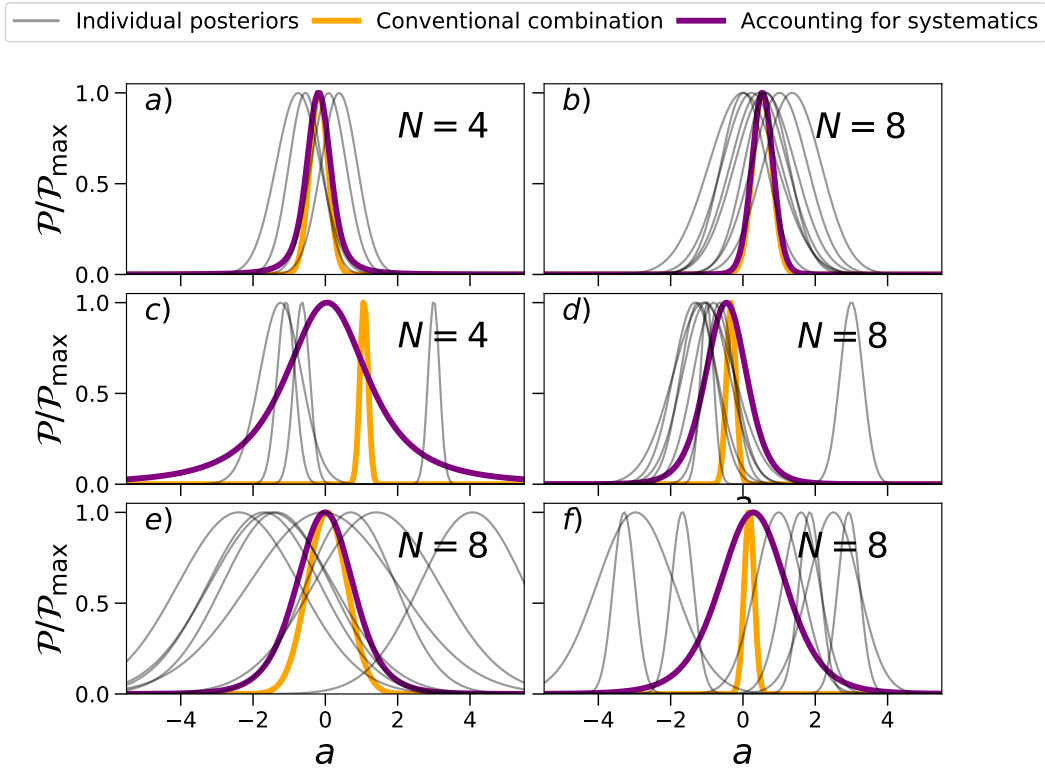


**Figure 2.** The same as Figure 1, but considering cases in which all the data sets are consistent (panels *a* and *b*), only one is discrepant with the rest (panels *c* and *d*), eight data sets with scatter larger than the errors (panel *e*) and eight data sets with random values of the best fit and errors (panel *f*).

$N = 3$ , etc., with an asymptotic dependence of  $(a/\epsilon)^{1-N}$  for  $N \gg 1$ . So, as in the previous case, the posterior cannot be normalized if  $N = 2$ , but it rapidly tends to a Gaussian for large  $N$ . This case is shown in the bottom panels of Figure 1. The appearance of these extended tails on the posterior is a characteristic result of our method, and seems inevitable if one is unwilling in advance to limit the size of possible shift systematics. The power-law form depends in detail on the hyperprior, but if we altered this by some power of  $\sigma_a$ , the result would be a different power-law form for the ‘fat tails’ still with the generic non-Gaussianity.

We also show in Figure 2 some more realistic examples, starting with mock consistent data that are drawn from a Gaussian using the assumed errors (rather than  $\tilde{a} = 0$ ), but then forcing one or more of these measurements to be discrepant. As with the simple  $\tilde{a} = 0$  example, we see that the results for several consistent data sets approach the conventional analysis for larger  $N$  (panels *a* and *b*). But when there is a single discrepant data set, the posterior is much broader than in the conventional case (panel *c*). Nevertheless, as the number of consistent data sets increases, the posterior shrinks to the point where it is only modestly broader than the conventional distribution, and where the single outlying measurement is clearly identified as discrepant (panel *d*). Thus our prior on the shifts, in which all measurements are assumed equally likely to be in error, does not prevent the identification of a case where there is a single rogue measurement. However, these examples do emphasize the desirability of having as many distinct classes of measurement as possible, even though this may mean resorting to measurements where the individual uncertainties are larger. Additional coarse information can play an important role in limiting the tails on the posterior, especially in cases where there are discordant data sets (see panel *d*). Finally, we also show examples where the scatter of the

individual best-fit is larger than the individual uncertainties of the data sets, so the size of the shifts are larger and our posterior is broader than the one obtained with conventional approach (panel *e*), and a case with several inconsistent measurements (with best-fit and errors distributed randomly), for which our posterior is centred close to 0 with a width set by the empirical distribution of the data (panel *f*).

### 3.2 Contrasting shift and rescaling parameters

If we ignore the constraints on  $\alpha_i$  and consider only the relative likelihoods (with width of the distribution determined by  $\sigma_i$ ), then there is an illuminating parallel between the effects of rescaling and shift parameters. Compare Equation 3.4, where all  $\alpha$  have been already marginalized over ( $\mathcal{P}_1$ ), with H02’s method ( $\mathcal{P}_2$ ):

$$\mathcal{P}_1 \propto \prod_i (\sigma_a^2 + \sigma_i^2)^{-1/2} \exp \left[ -\frac{1}{2} \sum_i \frac{(a - \tilde{a}_i)^2}{\sigma_a^2 + \sigma_i^2} \right]; \quad \mathcal{P}_2 \propto \prod_i \alpha_i^{1/2} \sigma_i^{-1} \exp \left[ -\frac{1}{2} \sum_i \frac{\alpha_i (a - \tilde{a}_i)^2}{\sigma_i^2} \right], \quad (3.6)$$

these two expressions are clearly the same if  $\alpha_i = (1 + \sigma_a^2/\sigma_i^2)^{-1}$ . However, there is a critical difference: while there is an  $\alpha_i$  for each class of experiments, we only consider a single  $\sigma_a$ , which participates in the prior for all the shift parameters of all classes of experiments.

On the other hand, if different  $\sigma_{\theta_j}$  for each data sets were to be used, this would be equivalent to a double use of rescaling parameters. Furthermore, in the case of having several experiments with inconsistent results, the posterior using only rescaling parameters would be a multimodal distribution peaked at the points corresponding to the individual posteriors, as seen in Figures 3 & 4 of H02. We feel that this is not a satisfactory outcome: it seems dangerously optimistic to believe that one out of a flawed set of experiments can be perfect when there is evidence that the majority of experiments are incorrect. Our aim should be to set conservative constraints, in which all experiments have to demonstrate empirically that they are *not* flawed (i.e. ‘guilty until proved innocent’).

### 3.3 Examples with multiple parameters

The approach to models with multiple parameters differs conceptually from the one-parameter case: there are several families of shifts,  $\{\Delta_\theta\}$ , with their corresponding covariance matrix. A convenient simple illustration is provided by the example chosen by H02: consider data sets sampled from different straight lines. Thus, the model under consideration is  $y = mx + c$ , where  $y$  &  $x$  are the information given by the data and  $m$  &  $c$  are the parameters to constrain.

We consider three different straight lines for which we sample the data,  $D_i$ :  $\{D_1\}$  and  $\{D_2\} \equiv \{m = c = 1\}$ ;  $\{D_3\} \equiv \{m = 0, c = 1.5\}$ ; and  $\{D_4\} \equiv \{m = c = 0.7\}$ . For all  $D_i$ , we consider three independent data sets (so  $N = 6$  when combining i.e.,  $D_1$  and  $D_2$ ) and assume  $\sigma_y = 0.1$  for every data point. We combine  $\{D_1\}$  with  $\{D_2\}$  in Figure 3, with  $\{D_3\}$  in Figure 4, and with  $\{D_4\}$  in Figure 5. Note the change of scale in each panel. In all cases, we study four situations corresponding to the combination of: all data sets with 50 or 5 points and errors correctly estimated or underestimated by a factor 5 (only in data sets from  $\{D_2\}$ ,  $\{D_3\}$  or  $\{D_4\}$ ). We use lognormal priors with  $b = -2$  and  $\xi = 16$  both for  $\sigma_m$  and  $\sigma_c$ , and a LKJ distribution with  $\eta = 1$  as the shifts hyperprior. We show the individual posteriors of each data set in black; the results using the conventional approach in orange; the constraints using only rescaling parameters in blue; using only shift parameters in purple; and using both in green. The occasional noisy shape of the latter is due to the numerical complexity of sampling the parameter space using rescaling and shifts. Generally, in this case the uncertainties are somewhat larger than in the case of using only shifts, except when individual errors are poorly estimated and the credible regions are much larger. This is because rescaling parameters gain a large weight in the analysis in order to recover a sensible  $\chi^2_{\nu,i}$ , which permits shifts that are too large for the corresponding prior (given that the corresponding likelihood is downweighted by small values of  $\alpha_i$ ). This can be seen comparing green and purple contours in the bottom panels of Figures 3, 4 & 5.

As can be seen in Figure 3, if the data sets are consistent and the errors are correctly estimated (top left panel), rescaling parameters have rather little effect on the final posterior. This supports our argument in Equation 3.2 and below. On the other hand, when errors are underestimated (bottom left



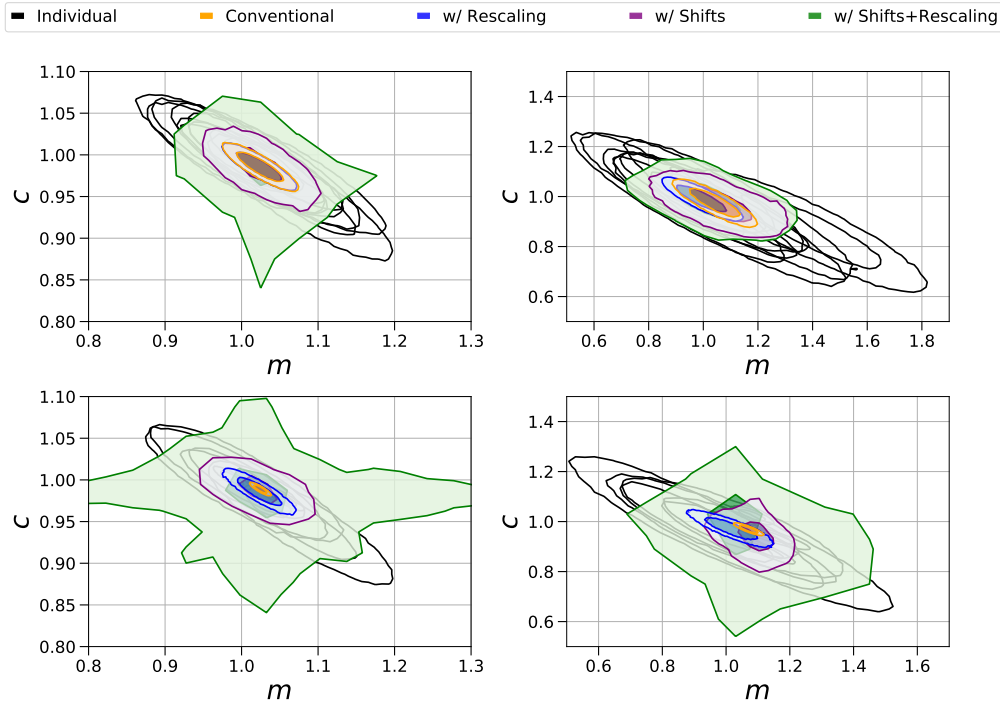


**Figure 3.** Constraints for six data sets sampled from a straight line with slope  $m = 1$  and intercept  $c = 1$  ( $\{D_1\}$  and  $\{D_2\}$ ). We show the individual posteriors in black and the results from using the conventional approach in orange, using rescaling parameters, in blue, using shift parameters, in purple, and using both in green. Top left: all data sets have 50 points. Top right: all data sets have 5 points. Bottom panels: as in the top panels, but the errors of  $\{D_2\}$  are underestimated a factor 5.

panel), the recovered posterior is similar to the one in which the errors are correctly estimated. When the data sets contain smaller number of points (right panels) the results are qualitatively similar.

As expected, rescaling parameters yield conservative constraints accounting for type 1 systematics, but it is not a good choice if the data sets are not consistent. As shown in Figures 4 & 5, the posterior for this case is multimodal, implying that the true values for the parameters are equally likely to correspond to one of the reported sets of values and ruling out values in between experiments, as foreshadowed in the previous section. Moreover, when the data sets are inconsistent and the errors of some of them underestimated, the constraints tend to favour only the values corresponding to such data sets (although with larger uncertainties than the conventional approach). Therefore, although rescaling parameters help to diagnose if any data set is suffering from both types of systematics, they cannot be used to obtain meaningful constraints if type 2 systematics are present.

On the other hand, using shift parameters gives constraints with larger uncertainties, allowing values between the results of the individual data sets and accepting the possibility that experiments might be polluted by unaccounted-for type 2 systematics (as it is the case in Figures 4 & 5). Surprisingly, they also provide correct conservative constraints when only type 1 systematics are present, with results similar to those obtained using only rescaling parameters (see, e.g., the bottom left panel of Figure 3).

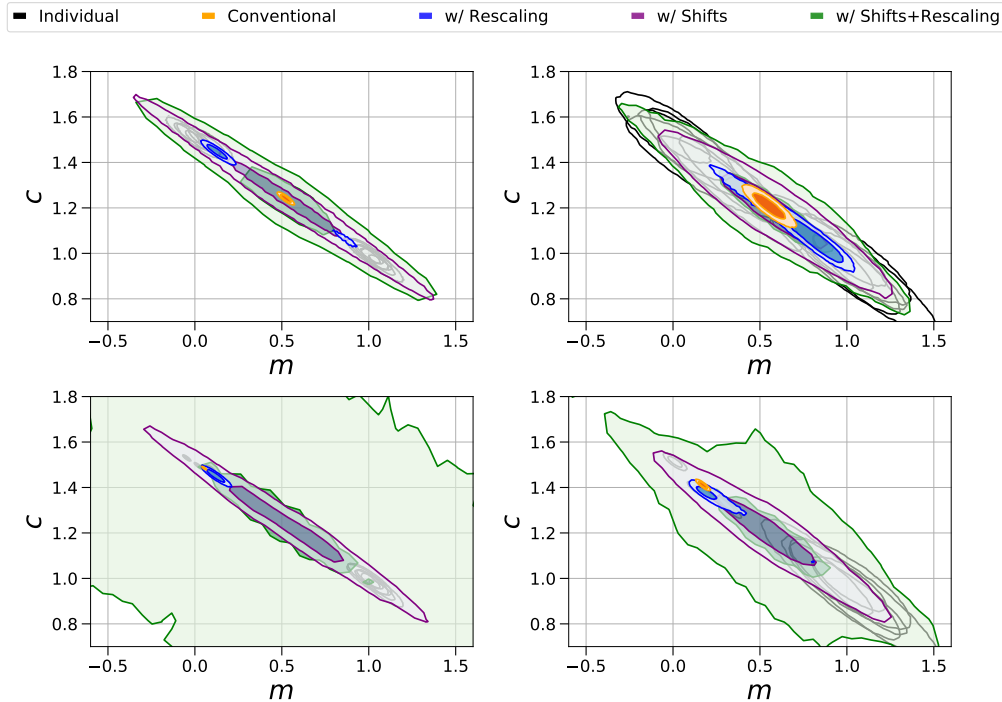


Figure 4. As Figure 3 but using  $\{D_3\}$  (with slope  $m = 0$  and intercept  $c = 1.5$ ) instead of  $\{D_2\}$ .

## 4 Applications to cosmology: $H_0$

In order to illustrate how our method performs in a problem of real interest, we apply it to the tensions in  $H_0$ . This tension has been studied from different perspectives in the literature. One of the options is to perform an independent analysis of the measurements to check for systematics in a concrete constraint, e.g., by including rescaling parameters to consider type 1 systematics in each measurement used to constrain  $H_0$  [24] or using a hierarchical analysis to model in more detail all the probability distribution functions [14]. Another possibility is to consider that this tension is a hint of new physics, rather than a product of unaccounted-for systematics, and therefore explore if other cosmological models ease it or if model independent approaches result in constraints that differ from the expectations of  $\Lambda$ CDM (see [25] and references therein).

Here we propose a third way. We consider all the existing independent constraints of  $H_0$  from low redshift observations and apply BACCUS to combine them and obtain a conservative joint constraint of  $H_0$ , accounting for any possible scale or shift systematic in each class of experiments (grouped as described in Section 4.1). We use only low redshift observations in order to have a consensus conservative constraint to confront with early Universe constraints from CMB observations. We assume a  $\Lambda$ CDM background expansion and use the cosmic distance ladder as in [26–28].

### 4.1 Data and modelling

In this section we describe the data included in the analysis. As discussed in Section 3.1, the size of the uncertainties using BACCUS are smaller for a larger number of classes of experiments, even if the individual errors are larger. Therefore, we include all independent constraints on  $H_0$  from low redshift observations available, independent of the size of their error bars. In principle, we should use the exact posterior reported by each experiment, but these are not always easily available. Therefore, we use the reported 68% credible limits in the case of the direct measurements of  $H_0$ , assuming a

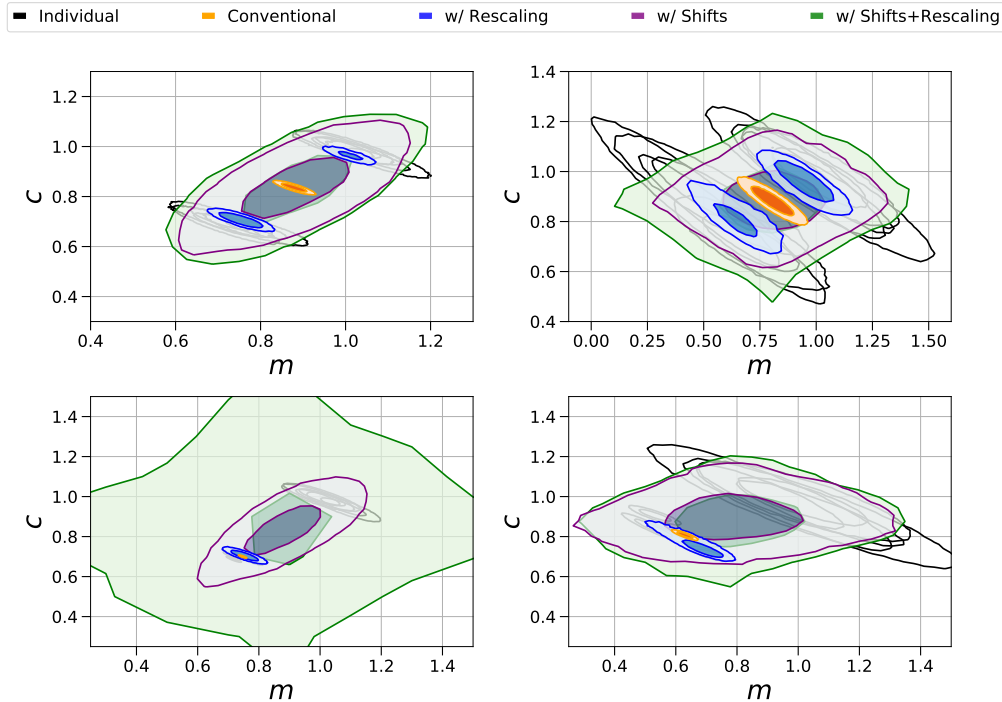


**Figure 5.** As Figure 3 but using  $\{D_4\}$  (with slope  $m = 0.7$  and intercept  $c = 0.7$ ) instead of  $\{D_2\}$ .

Gaussian likelihood. The resulting error in the tails of the posterior is one form of systematic, which BACCUS should be able to absorb. The different classes of experiments are grouped as described below:

- **Direct measurements using the distance ladder.** We include as different classes of experiments direct measurements that use different standard candles or distance anchors. These are: the three independent measurements used in Riess et al. 2016 (see table 6 in [4]), the relation between the integrated  $H\beta$  line luminosity and the velocity dispersion of the ionized gas in HII galaxies and giant HII regions [29], megamasers [30–32] and the  $H_0$  value measured by the Cosmic Flows project [33]. Finally, we use the direct measurement coming from the standard siren [34] from the neutron star merger whose gravitational wave was detected by VIRGO and LIGO collaborations [35] and whose electromagnetic counterpart was also detected by several telescopes [36]. We do not include the measurement using the Tip of the Red Giant Branch from [37] because such analysis uses anchors and measurements included in the analysis of Riess et al. (2016) [4].
- **Baryon Acoustic Oscillations (BAO).** Assuming an underlying expansion history, BAO measurements constrain the low redshift standard ruler,  $r_s h$  (see e.g. [28]), where  $r_s$  is the sound horizon at radiation drag and  $h = H_0/100$ . Measurements of the primordial deuterium abundance can be used to break this degeneracy [38, 39], given that they can be used to infer the physical density of baryons,  $\Omega_b h^2$  [40]. We use BAO measurements from the following galaxy surveys: Six Degree Field Galaxy Survey (6dF) [41], the Main Galaxy Sample of Data Release 7 of Sloan Digital Sky Survey (SDSS-MGS) [42], the galaxy sample of Baryon Oscillation Spectroscopic Survey Data Release 12 (BOSS DR12) [2], the Lyman- $\alpha$  forest autocorrelation from BOSS DR12 [43] and their cross correlation with quasars [44], the reanalysed measurements of WiggleZ [45], and the measurement using quasars at  $z = 1.52$  [46]. We use anisotropic measurements when available (including their covariance) and account for the covariance between

the different redshift bins within the same survey when needed. We consider BOSS DR12 and WiggleZ measurements as independent because the overlap of both surveys is very small, hence their correlation (always below 4%) can be neglected [47, 48]. For our analysis, we consider observations of different surveys or tracers (i.e., the autocorrelation of the Lyman- $\alpha$  forest and its cross correlation with quasars are subject to different systematics) as different classes of experiments.

- **Time delay distances.** Using the time delays from the different images of strong lensed quasars it is possible to obtain a good constraint on  $H_0$  by using the time delay distance if an expansion history is assumed. We use the three measurements of the H0LiCOW project [49] as a single class of experiment
- **Cosmic clocks.** Differential ages of old elliptical galaxies provide estimate of the inverse of the Hubble parameter,  $H(z)^{-1}$  [50]. We use a compilation of cosmic clocks measurements including the measurement of [51], which extends the prior compilation to include both a fine sampling at  $0.38 < z < 0.48$  using BOSS Data Release 9, and the redshift range up to  $z \sim 2$ . As all cosmic clock measurements have been obtained from the same group using similar analyses, we consider the whole compilation as a single class of experiment.
- **Supernovae Type Ia.** As we want to focus mostly on  $H_0$ , we use the Joint Light curve Analysis (JLA) of Supernovae Type Ia [3] as a single class of experiment to constrain the unnormalized expansion history  $E(z) = H(z)/H_0$ , hence tighter constraints on the matter density parameter,  $\Omega_M$ , are obtained.

We do not consider the assumption of a  $\Lambda$ CDM-like expansion history (which connects BAO, time delay distances, cosmic clocks and supernovae) as a source of systematic errors which couples different class of experiments (since it affects each observable in a different way). Therefore, we can neglect any correlation among these four probes. In order to interpret the above experiments, we need a model that contains three free parameters:  $H_0$ ,  $\Omega_c h^2$ , and  $\Omega_b h^2$ .  $\Omega_b h^2$  will only be constrained by a prior coming from [40] and, together with  $\Omega_c h^2$  and  $H_0$ , allows us to compute  $r_s$  and break the degeneracy between  $H_0$  and  $r_s$  in BAO measurements. As we focus on  $H_0$  and variations in  $\Omega_b h^2$  do not affect  $E(z)$  significantly, we do not apply any shift to  $\Omega_b h^2$ . We compute a grid of values of  $100 \times r_s h$  for different values of  $H_0$ ,  $\Omega_c h^2$  and  $\Omega_b h^2$  using the public Boltzmann code CLASS [52, 53] before running the analysis and interpolate the values at each step of the MCMC to obtain  $r_s$  in a rapid manner<sup>2</sup>.

## 4.2 Results

In this section we show the results using BACCUS when addressing the tension in  $H_0$ . We compare them with the results obtained using the conventional approach and the methodology introduced in H02. First, we consider marginalized measurements of  $H_0$ . Ideally, we would apply BACCUS to Riess et al. 2016 and Planck measurements. However, as stated in Section 2, this method can not be applied to only two measurements. Thus, we use the independent and much broader measurement coming from the neutron star merger [34] in order to constrain the tails of the final posterior. These results can be found in Figure 6. Even with the inclusion of a third measurement, the tails of the posterior when shift parameters are added are still too large and therefore the conservative constraints are very weak (due to the low number of experiments included). On the other hand, adding only rescaling parameters results in a bimodal distribution. In order to obtain relevant conservative constraints, more observations need to be included in the analysis.

As the next step, we perform an analysis with more data and compare the results of the different methodologies to the combination of the data listed in Table 1, as recently used in [54]. Since marginalized constraints in clear tension are combined, this is a case where BACCUS is clearly necessary. We use the lognormal hyperprior with  $b = -2$  and  $\xi = 16$  for the hyperprior of variance of the shifts in both cases.

<sup>2</sup>We make a grid for  $100 \times r_s h$  in order to minimize the error in the interpolation ( $\lesssim 0.1\%$ ). This grid is available upon request.

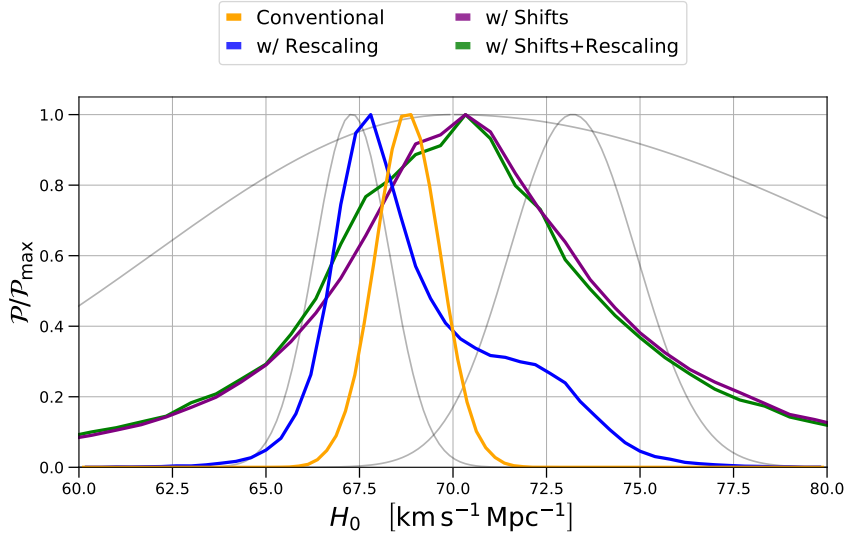


**Figure 6.** Marginalized  $H_0$  posterior distributions obtained from the combination of marginalized  $H_0$  constraints from the local measurement of Riess et al. 2016, Planck and the neutron star merger. We show results with the standard approach (orange), with only rescaling (blue), with only shifts (purple) and with both rescaling and shifts (green).

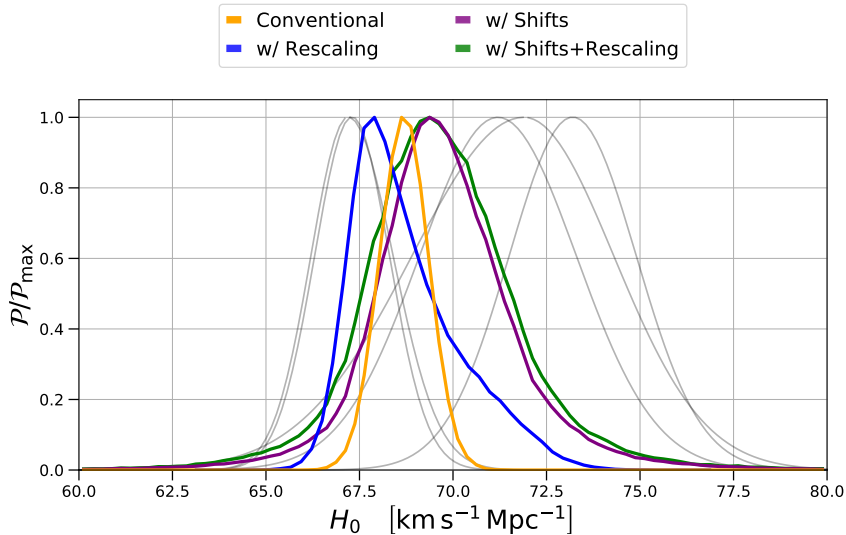


**Figure 7.** Marginalized  $H_0$  posterior distributions obtained from the combination of marginalized  $H_0$  constraints from the experiments listed in Table 1. We show results with the standard approach (orange), with only rescaling (blue), with only shifts (purple) and with both rescaling and shifts (green).

The results of this comparison can be found in Figure 7 and Table 1, where we report the marginalized highest posterior density values and 68% (95% in parenthesis) credible limits and the individual measurements used. As expected, the results using BACCUS peak among the individual best fits and have larger uncertainties than using the conventional approach. However, comparing with the individual constraints, the result seems more sensible. There is a small difference between the combined result reported in [54] and our result using the conventional approach due to using different samplers.

	Experiment/Approach	$H_0$ (km s <sup>-1</sup> Mpc <sup>-1</sup> )
Individual Measurements	DES[54]	$67.2^{+1.2}_{-1.0}$
	Planck [1]	$67.3 \pm 1.0$
	SPTpol [55]	$71.2 \pm 2.1$
	H0LiCOW [49]	$71.9^{+2.4}_{-3.0}$
	Riess et al. 2016 [4]	$73.2 \pm 1.7$
This work	Conventional combination	$68.7 \pm 0.6(\pm 1.2)$
	Rescaling param.	$67.8^{+1.8(+4.1)}_{-0.6(-1.3)}$
	Shift param.	$69.5^{+1.7(+4.7)}_{-1.4(-3.4)}$
	Shift + rescaling param.	$69.4^{+2.1(+4.9)}_{-1.4(-3.8)}$

**Table 1.** Individual marginalized constraints on  $H_0$  combined to evaluate the performance of our method in a real one dimensional problem. In the bottom part, we report highest posterior density values and 68% (95% in parenthesis) credible limits obtained combining the individual measurement using different kind of parameters.

Approach	$H_0$ (km s <sup>-1</sup> Mpc <sup>-1</sup> )	$\Omega_M$
Conventional combination	$70.15^{+0.5(+1.3)}_{-0.6(-1.4)}$	$0.32 \pm 0.01(\pm 0.03)$
Rescaling param.	$69.4 \pm 0.7(\pm 1.5)$	$0.32 \pm 0.01(\pm 0.03)$
Shift param. (only $H_0$ )	$70.6^{+0.8(+1.9)}_{-1.1(-2.3)}$	$0.31 \pm -0.02(\pm 0.04)$
Shift (only $H_0$ ) + rescaling param.	$70.5^{+0.9(+2.6)}_{-1.3(-3.1)}$	$0.31 \pm -0.02(^{+0.04}_{-0.05})$
Shift param. ( $H_0$ & $\Omega_M$ )	$71.7^{+0.8(+2.0)}_{-1.2(-2.8)}$	$0.33 \pm 0.04(^{+0.09}_{-0.07})$
Shift ( $H_0$ & $\Omega_M$ ) + rescaling param.	$71.0^{+1.8(+3.6)}_{-0.9(-5.4)}$	$0.33^{+0.02(+0.12)}_{-0.04(-0.14)}$

**Table 2.** Highest posterior density values and 68% (95% in parenthesis) credible level marginalized constraints of  $H_0$  and  $\Omega_M$  obtained using the data and methodology described in Section 4.1.

We now apply our method to the data described in Section 4.1 to obtain conservative limits on  $H_0$  using all the available independent low redshift observations. Regarding the introduction of shift parameters, we consider two cases. In the first case (shown in Figure 8) we only use them on  $H_0$ ,  $\Delta_H$ . On the other hand, in the second case (shown in Figure 9) we also use them on  $\Omega_c h^2$ ,  $\Delta_\Omega$ . In both cases, rescaling parameters are applied to every class of experiments and we use the same parameters as in the previous case for the hyperprior for  $\sigma_H$  and a lognormal distribution with  $b = -4$  and  $\xi = 9$  as the hyperprior for  $\sigma_\Omega$ . We use  $\eta = 1$  for the LKJ hyperprior of the correlation. Marginalized credible limits from both cases can be found in Table 2.

As there is no inconsistency in  $\Omega_M$  among the experiments (given that most of the constraints are very weak) the only effect of including  $\Delta_\Omega$  in the marginalized constraints in  $\Omega_M$  is to broaden the posteriors. In contrast, including  $\Delta_H$  shifts the peak of the  $H_0$  marginalized posterior. While the tightest individual constraints correspond to low values of  $H_0$  (BAO and cosmic clocks), BACCUS favours slightly larger values than the conventional approach (which stays in the middle of the tension, as expected). These effects are larger when we include  $\Delta_\Omega$ , given that there is more freedom in the parameter space. On the other hand, as BAO and cosmic clocks are the largest data sets, the analysis with only rescaling parameters prefers a lower  $H_0$ . Nonetheless, as the constraints weaken when

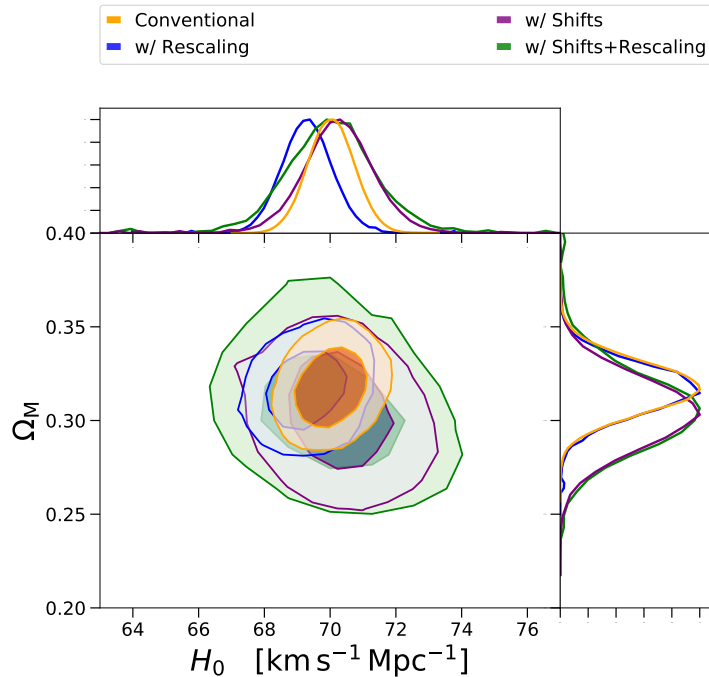


**Figure 8.** 68% and 95% credible level marginalized constraints on the  $H_0$ - $\Omega_M$  plane using different methods. We show results with the standard approach (orange), with only rescaling parameters (blue), with only shift parameters (purple) and with both rescaling and shifts (green). Shifts are applied only to  $H_0$ .

introducing shifts and rescaling, all these modifications are not of great statistical significance.

When including only  $\Delta_H$ , there is an effect on both the constraints on  $H_0$  and also on  $\Omega_M$  (both slightly shifting the maximum and broadening the errors), due to the small correlation between the two parameters. The behaviour of the marginalized constraints on  $H_0$  is similar to the one discussed above. However, when both  $\Delta_H$  and  $\Delta_\Omega$  are included, the constraints are much weaker than in the previous case. Including shifts for  $\Omega_c h^2$  also increases the uncertainties in the marginalized constraints on  $H_0$ . Nonetheless, it is important to bear in mind that the data used in this analysis constrain  $H_0$  much better than they do  $\Omega_M$ , even using the conventional approach. Finally, note that in this case the constraints including both shift and rescaling parameters and those using only shifts are not very different (in contrast to the cases showed in Figures 3, 4 & 5), since here the type 1 systematic errors are well accounted for and individual  $\chi_\nu^2 \simeq 1$ .

Regarding the ability of BACCUS to spot which data set is more likely to be affected by systematics, there is not a clear answer for this specific problem. This is because more independent data is needed in order to discriminate between different classes of experiments, given the inconsistencies within the data sets listed in Section 4.1.

## 5 Summary and discussion

In this paper, we have considered the increasingly common issue of statistical tensions in the results of cosmological experiments: small inconsistencies in estimated parameters that are of marginal sig-

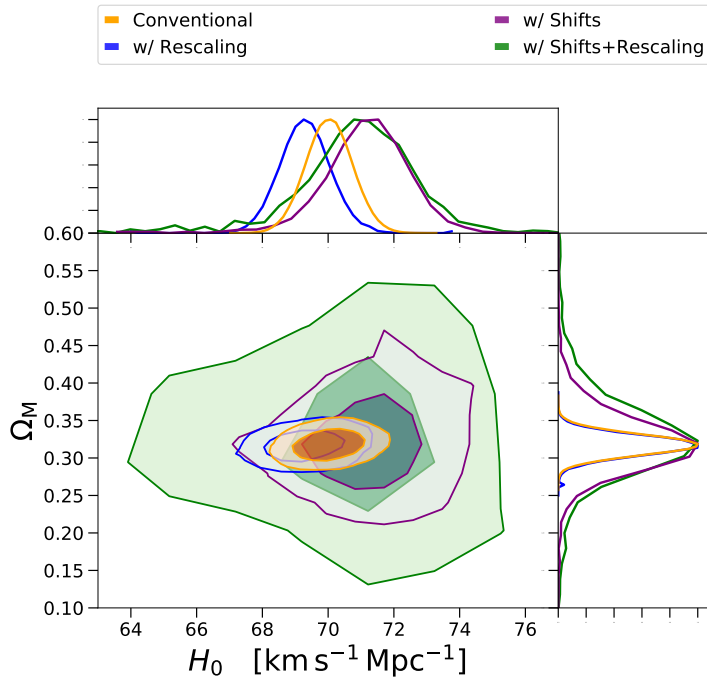


**Figure 9.** Same as Figure 8 but in this case the shifts are applied to both  $H_0$  and  $\Omega_c h^2$ . Note the change of scale in the vertical axis.

nificance, but which are too large for comfort. In this case, we face the statistical question of how to combine data sets that are in tension, in order to obtain parameter constraints that are robust. If there are ‘unknown unknowns’ in the data or the theory, then the standard analysis of the combined constraints on model parameters may not be reliable – which in turn risks erroneous claims of new physics in a distinct way. This is indeed a statistical issue that is not confined to cosmology: similar challenges arise elsewhere in astrophysics (e.g. [56]), and analogous challenges can be encountered in particle physics experiments.

In response to this situation, we have introduced **BACCUS**, a method for combining data for parameter inference in a conservative and agnostic way that allows consistently for the possible presence of unknown systematics in the data sets. It deals not only with systematics arising from incorrect estimation of the magnitude of random measurement errors (already considered by Hobson et al. 2002; H02), but also with those systematics whose effect is such that the inferred model parameters are biased with respect to the true values. The latter are the truly dangerous systematics, since they cannot be detected by any internal null test of a single experiment. In order to account for such effects, we introduce ‘shift’ parameters,  $\{\Delta_{\theta}\}$ , which offset the best-fitting model parameters for each set of data independent from the rest. The magnitude of such offsets can be constrained by inspecting the degree of agreement between different data sets, and conservative posteriors on parameters can be inferred by marginalizing over the offsets.

Our approach is democratic and also pessimistic: we assume that all experiments are equally likely to suffer from shift systematics of similar magnitude, independent of their quoted statistical precision, and we are reluctant to set an upper limit to the size of possible systematics. Crucially,



therefore, the prior for the shifts should take no account of the size of the reported random errors, since shift systematics by definition cannot be diagnosed internally to an experiment, however precise it may be. In practice, we assume that the shifts have a Gaussian distribution, with a prior characterised by some unknown covariance matrix. We adopt a separation strategy to address the hyperprior for this covariance, using the LKJ distribution for the correlations and independent lognormal distributions for the standard deviations. We recommend agnostic wide hyperpriors, preferring to see explicitly how data can rein in the possibility of arbitrarily large systematics.

For each data set, the shift parameters are assumed to be drawn independently from the same prior. But this assumption is not valid when considering independent experiments that use the same technique, since they may well all suffer from systematics that are common to that method. Therefore data should first be combined into different *classes* of experiments before applying our method. In practice, however, a single experiment may use a number of methods that are substantially independent (e.g. the use of lensing correlations and angular clustering by DES). In that case, our approach can be similarly applied to obtain conservative constraints and assess internal consistency of the various sub-methods.

Because it is common for joint posterior distributions to display approximate degeneracies between some parameters, a systematic that affects one parameter may induce an important shift in others. For example, in Figure 8 the probability density function of  $\Omega_M$  changes due to  $\Delta_H$ . For complicated posteriors, it is therefore better in principle to use our approach at the level of the analysis of the data (where all the model parameters are varied), rather than constructing marginalized constraints on a single parameter of interest and only then considering systematics.

These assumptions could be varied: in some cases there could be enough evidence to consider certain experiments more reliable than others, so that the prior for the shifts will not be universal. But recalling the discussion in 3.1 concerning the use of different shift priors for each data sets, a way to proceed might be to rescale  $\sigma_{\theta_j}$  only for certain data sets (those more trusted), but then to use the same prior for all data sets after rescaling. If we consider the data sets  $D_{i'}$  to be more reliable than the rest, the final prior should be

$$\mathcal{P}(\Delta_a|\sigma_a) \propto \frac{1}{\sigma_a^{N-1}} \exp \left[ -\frac{1}{2} \sum_{i \neq i'}^N (\Delta_a^i/\sigma_a)^2 \right] \frac{1}{\sigma_a/\beta} \exp \left[ -\frac{1}{2} (\Delta_a^{i'}/(\sigma_a/\beta))^2 \right], \quad (5.1)$$

where we consider the case with only one parameter  $a$  for clarity and  $\beta$  is a constant  $> 1$ .

Another possibility is to weaken the assumption that arbitrarily bad shift systematics are possible. One can achieve this either by imposing explicit limits so that the shifts never take values beyond the chosen bound, or by altering the prior on the shift parameters, making it narrower. Although the methodology is sufficiently flexible to accommodate such customizations, we have preferred to keep the assumptions as few and simple as possible. As we have seen, large shifts are automatically disfavoured as the number of concordant data sets rises, and this seems a better way to achieve the outcome.

It is also possible to ascertain if a single experiment is affected by atypically large shifts, by inspecting the marginalized posteriors for the shifts applicable to each dataset. A straightforward option now is to compute the relative Bayesian evidence between the models with and without shifts, telling us how strongly we need to include them, as done in H02. But this procedure needs care: consider a model with many parameters but only one,  $\theta_j$ , strongly affected by type 2 systematics. In that case, the evidence ratio will favour the model without shifts, those not affecting  $\theta_j$  are not necessary. Therefore, the ideal procedure is to check the evidence ratio between models with different sets of families of shifts, although this is computationally demanding.

After applying our method to some simple example models and comparing it with the scaling of reported errors as advocated by H02, we have applied it to a real case in cosmology: the tension in  $H_0$ . In general,  $H_0$  values obtained in this way are larger than either those from the conventional approach, or the combination using the approach of H02. However, as our conservative uncertainties are larger there is no tension when compared with the CMB value inferred assuming  $\Lambda$ CDM. We have focused on the application to parameter inference by shifting the model parameters for each data set.

However, it is also possible to apply the same approach to each individual measurement of a data set, in the manner that rescaling parameters were used by [24].

We may expect that the issues explored here will continue to generate debate in the future. Next-generation surveys will witness improvements of an order of magnitude in precision, yielding statistical errors that are smaller than currently known systematics. Great efforts will be invested in refining methods for treating these known problems, but the smaller the statistical errors become, the more we risk falling victim to unknown systematics. In the analysis presented here, we have shown how allowance can be made for these, in order to yield error bounds on model parameters that are conservative. We can hardly claim our method to be perfect: there is always the possibility of global errors in basic assumptions that will be in common between apparently independent methods. Even so, we have shown that realistic credibility intervals can be much broader than the formal ones derived using standard methods. But we would not want to end with a too pessimistic conclusion: the degradation of precision need not be substantial provided we have a number of independent methods, and provided they are in good concordance. As we have seen, a conservative treatment will nevertheless leave us with extended tails to the posterior, so there is an important role to be played by pursuing a number of independent techniques of lower formal precision. In this way, we can obtain the best of both worlds: the accuracy of the best experiments, and reassurance that these have not been rendered unreliable by unknown unknowns.

Finally, a possible criticism of our approach is that an arms-length meta-analysis is no substitute for the hard work of becoming deeply embedded in a given experiment to the point where all systematics are understood and rooted out. We would not dispute this, and do not wish our approach to be seen as encouraging lower standards of internal statistical rigour; at best, it is a means of taking stock of existing results before planning the next steps. But we believe our analysis is useful in indicating how the community can succeed in its efforts.

## Acknowledgments

We thank Licia Verde and Charles Jenkins for useful discussion during the development of this work, and Alan Heavens, Andrew Liddle, & Mike Hobson for comments which help to improve this manuscript. Funding for this work was partially provided by the Spanish MINECO under projects AYA2014-58747-P AEI/FEDER UE and MDM-2014-0369 of ICCUB (Unidad de Excelencia Maria de Maeztu). JLB is supported by the Spanish MINECO under grant BES-2015-071307, co-funded by the ESF. JLB thanks the Royal Observatory Edinburgh at the University of Edinburgh for hospitality. JAP is supported by the European Research Council, under grant no. 670193 (the COSFORM project).

## References

- [1] **Planck** Collaboration, P. A. R. Ade *et al.*, “Planck 2015 results. XIII. Cosmological parameters,” [arXiv:1502.01589 \[astro-ph.CO\]](#).
- [2] **SDSS-III BOSS** Collaboration, S. Alam and *et al.*, “The clustering of galaxies in the completed SDSS-III Baryon Oscillation Spectroscopic Survey: cosmological analysis of the DR12 galaxy sample,” [MNRAS](#) **470** (Sept., 2017) 2617–2652, [arXiv:1607.03155](#).
- [3] M. Betoule *et al.*, “Improved cosmological constraints from a joint analysis of the SDSS-II and SNLS supernova samples,” [Astron. Astrophys.](#) **568** (Aug., 2014) A22, [arXiv:1401.4064](#).
- [4] A. G. Riess, L. M. Macri, S. L. Hoffmann, D. Scolnic, S. Casertano, A. V. Filippenko, B. E. Tucker, M. J. Reid, D. O. Jones, J. M. Silverman, R. Chornock, P. Challis, W. Yuan, P. J. Brown, and R. J. Foley, “A 2.4% Determination of the Local Value of the Hubble Constant,” [ApJ](#) **826** (July, 2016) 56, [arXiv:1604.01424](#).
- [5] H. Hildebrandt and V. *et al.*, “KiDS-450: cosmological parameter constraints from tomographic weak gravitational lensing,” [Mon. Not. Roy. Astron. Soc.](#) **465** (Feb., 2017) 1454–1498, [arXiv:1606.05338](#).
- [6] DES Collaboration and e. a. Abbott, “Dark Energy Survey Year 1 Results: Cosmological Constraints from Galaxy Clustering and Weak Lensing,” [ArXiv e-prints](#) (Aug., 2017) , [arXiv:1708.01530](#).

- [7] A. Heavens, Y. Fantaye, E. Sellentin, H. Eggers, Z. Hosenie, S. Kroon, and A. Mootoivaloo, “No Evidence for Extensions to the Standard Cosmological Model,” [\*Physical Review Letters\* \*\*119\*\* no. 10, \(Sept., 2017\) 101301](#), [arXiv:1704.03467](#).
- [8] P. Marshall, N. Rajguru, and A. Slosar, “Bayesian evidence as a tool for comparing datasets,” [\*Phys. Rev. D\* \*\*73\*\* no. 6, \(Mar., 2006\) 067302](#), [astro-ph/0412535](#).
- [9] L. Verde, P. Protopapas, and R. Jimenez, “Planck and the local Universe: Quantifying the tension,” [\*Physics of the Dark Universe\* \*\*2\*\* \(Sept., 2013\) 166–175](#), [arXiv:1306.6766](#) [[astro-ph.CO](#)].
- [10] S. Seehars, A. Amara, A. Refregier, A. Paranjape, and J. Akeret, “Information gains from cosmic microwave background experiments,” [\*Phys. Rev. D\* \*\*90\*\* no. 2, \(July, 2014\) 023533](#), [arXiv:1402.3593](#).
- [11] T. Charnock, R. A. Battye, and A. Moss, “Planck data versus large scale structure: Methods to quantify discordance,” [\*Phys. Rev. D\* \*\*95\*\* no. 12, \(June, 2017\) 123535](#), [arXiv:1703.05959](#).
- [12] W. Lin and M. Ishak, “Cosmological discordances: A new measure, marginalization effects, and application to geometry versus growth current data sets,” [\*Phys. Rev. D\* \*\*96\*\* no. 2, \(July, 2017\) 023532](#), [arXiv:1705.05303](#).
- [13] S. M. Feeney, H. V. Peiris, A. R. Williamson, S. M. Nissanke, D. J. Mortlock, J. Alsing, and D. Scolnic, “Prospects for resolving the Hubble constant tension with standard sirens,” [ArXiv e-prints](#) (Feb., 2018), [arXiv:1802.03404](#).
- [14] S. M. Feeney, D. J. Mortlock, and N. Dalmaso, “Clarifying the Hubble constant tension with a Bayesian hierarchical model of the local distance ladder,” [ArXiv e-prints](#) (June, 2017), [arXiv:1707.00007](#).
- [15] J. Alsing, A. Heavens, and A. H. Jaffe, “Cosmological parameters, shear maps and power spectra from CFHTLenS using Bayesian hierarchical inference,” [\*Mon. Not. Roy. Astron. Soc.\* \*\*466\*\* \(Apr., 2017\) 3272–3292](#), [arXiv:1607.00008](#).
- [16] W. H. Press, “Understanding data better with Bayesian and global statistical methods.,” in [Unsolved Problems in Astrophysics](#), J. N. Bahcall and J. P. Ostriker, eds., pp. 49–60. 1997. [astro-ph/9604126](#).
- [17] O. Lahav, S. L. Bridle, M. P. Hobson, A. N. Lasenby, and L. Sodr e, “Bayesian ‘hyper-parameters’ approach to joint estimation: the Hubble constant from CMB measurements,” [\*Mon. Not. Roy. Astron. Soc.\* \*\*315\*\* \(July, 2000\) L45–L49](#), [astro-ph/9912105](#).
- [18] M. P. Hobson, S. L. Bridle, and O. Lahav, “Combining cosmological data sets: hyperparameters and Bayesian evidence,” [\*Mon. Not. Roy. Astron. Soc.\* \*\*335\*\* \(Sept., 2002\) 377–388](#), [astro-ph/0203259](#).
- [19] D. Foreman-Mackey, D. W. Hogg, D. Lang, and J. Goodman, “emcee: The MCMC Hammer,” [\*Publications of the Astronomical Society of the Pacific\* \*\*125\*\* \(Mar., 2013\) 306–312](#), [arXiv:1202.3665](#) [[astro-ph.IM](#)].
- [20] Y.-Z. Ma and A. Bernds en, “How to combine correlated data sets—A Bayesian hyperparameter matrix method,” [\*Astronomy and Computing\* \*\*5\*\* \(July, 2014\) 45–56](#), [arXiv:1309.3271](#) [[astro-ph.IM](#)].
- [21] I. Alvarez, J. Niemi, and M. Simpson, “Bayesian inference for a covariance matrix,” [Annual Conference on Applied Statistics in Agriculture](#) **26** (2014) 71–82, [arXiv:1408.4050](#) [[stat.ME](#)].
- [22] J. Barnard, R. McCulloch, and X. L. Meng, “Modeling covariance matrices in terms of standard deviations and correlations, with application to shrinkage,” [\*Statistica Sinica\* \*\*10\*\*\(4\) \(Oct., 2000\) 1281–1311](#).
- [23] D. Lewandowski, D. Kurowicka, and H. Joe, “Generating random correlation matrices based on vines and extended onion method,” [\*Journal of Multivariate Analysis\* \*\*100\*\*\(9\) \(2009\) 1989–2001](#).
- [24] W. Cardona, M. Kunz, and V. Pettorino, “Determining  $H_0$  with Bayesian hyper-parameters,” [\*JCAP\* \*\*3\*\* \(Mar., 2017\) 056](#), [arXiv:1611.06088](#).
- [25] J. L. Bernal, L. Verde, and A. G. Riess, “The trouble with  $H_0$ ,” [\*JCAP\* \*\*10\*\* \(Oct., 2016\) 019](#), [arXiv:1607.05617](#).
- [26] A. Heavens, R. Jimenez, and L. Verde, “Standard rulers, candles, and clocks from the low-redshift Universe,” [\*Phys. Rev. Lett.\* \*\*113\*\* no. 24, \(2014\) 241302](#), [arXiv:1409.6217](#) [[astro-ph.CO](#)].
- [27] A. J. Cuesta, L. Verde, A. Riess, and R. Jimenez, “Calibrating the cosmic distance scale ladder: the

- role of the sound horizon scale and the local expansion rate as distance anchors,” [Mon. Not. Roy. Astron. Soc. \*\*448\*\* no. 4, \(2015\) 3463–3471](#), [arXiv:1411.1094 \[astro-ph.CO\]](#).
- [28] L. Verde, J. L. Bernal, A. F. Heavens, and R. Jimenez, “The length of the low-redshift standard ruler,” [MNRAS \*\*467\*\* \(May, 2017\) 731–736](#), [arXiv:1607.05297](#).
- [29] D. Fernández-Arenas, E. Terlevich, R. Terlevich, J. Melnick, R. Chávez, F. Bresolin, E. Telles, M. Plionis, and S. Basilakos, “An independent determination of the local Hubble constant,” [ArXiv e-prints \(Oct., 2017\)](#), [arXiv:1710.05951](#).
- [30] M. J. Reid, J. A. Braatz, J. J. Condon, K. Y. Lo, C. Y. Kuo, C. M. V. Impellizzeri, and C. Henkel, “The Megamaser Cosmology Project. IV. A Direct Measurement of the Hubble Constant from UGC 3789,” [Astrophys. J. \*\*767\*\* \(Apr., 2013\) 154](#), [arXiv:1207.7292](#).
- [31] C. Y. Kuo, J. A. Braatz, K. Y. Lo, M. J. Reid, S. H. Suyu, D. W. Pesce, J. J. Condon, C. Henkel, and C. M. V. Impellizzeri, “The Megamaser Cosmology Project. VI. Observations of NGC 6323,” [Astrophys. J. \*\*800\*\* \(Feb., 2015\) 26](#), [arXiv:1411.5106](#).
- [32] F. Gao, J. A. Braatz, M. J. Reid, K. Y. Lo, J. J. Condon, C. Henkel, C. Y. Kuo, C. M. V. Impellizzeri, D. W. Pesce, and W. Zhao, “The Megamaser Cosmology Project. VIII. A Geometric Distance to NGC 5765b,” [Astrophys. J. \*\*817\*\* \(Feb., 2016\) 128](#), [arXiv:1511.08311](#).
- [33] R. B. Tully, H. M. Courtois, and J. G. Sorce, “Cosmicflows-3,” [Astrophys. J. \*\*152\*\* \(Aug., 2016\) 50](#), [arXiv:1605.01765](#).
- [34] B. P. Abbott, R. Abbott, T. D. Abbott, F. Acernese, K. Ackley, C. Adams, T. Adams, P. Addesso, R. X. Adhikari, V. B. Adya, and et al., “A gravitational-wave standard siren measurement of the Hubble constant,” [ArXiv e-prints \(Oct., 2017\)](#), [arXiv:1710.05835](#).
- [35] B. P. Abbott, R. Abbott, T. D. Abbott, F. Acernese, K. Ackley, C. Adams, T. Adams, P. Addesso, R. X. Adhikari, V. B. Adya, and et al., “GW170817: Observation of Gravitational Waves from a Binary Neutron Star Inspiral,” [Physical Review Letters \*\*119\*\* no. 16, \(Oct., 2017\) 161101](#), [arXiv:1710.05832 \[gr-qc\]](#).
- [36] B. P. Abbott, R. Abbott, T. D. Abbott, F. Acernese, K. Ackley, C. Adams, T. Adams, P. Addesso, R. X. Adhikari, V. B. Adya, and et al., “Multi-messenger Observations of a Binary Neutron Star Merger,” [Astrophys. J. Letters \*\*848\*\* \(Oct., 2017\) L12](#), [arXiv:1710.05833 \[astro-ph.HE\]](#).
- [37] I. S. Jang and M. G. Lee, “The Tip of the Red Giant Branch Distances to Type Ia Supernova Host Galaxies. V. NGC 3021, NGC 3370, and NGC 1309 and the value of the Hubble Constant,” [ArXiv e-prints \(Feb., 2017\)](#), [arXiv:1702.01118](#).
- [38] G. E. Addison, G. Hinshaw, and M. Halpern, “Cosmological constraints from baryon acoustic oscillations and clustering of large-scale structure,” [MNRAS \*\*436\*\* \(Dec., 2013\) 1674–1683](#), [arXiv:1304.6984](#).
- [39] É. Aubourg et al., “Cosmological implications of baryon acoustic oscillation measurements,” [Phys. Rev. D \*\*92\*\* no. 12, \(Dec., 2015\) 123516](#), [arXiv:1411.1074](#).
- [40] R. Cooke, M. Pettini, and C. C. Steidel, “A one percent determination of the primordial deuterium abundance,” [ArXiv e-prints \(Oct., 2017\)](#), [arXiv:1710.11129](#).
- [41] F. Beutler, C. Blake, M. Colless, D. H. Jones, L. Staveley-Smith, L. Campbell, Q. Parker, W. Saunders, and F. Watson, “The 6dF Galaxy Survey: baryon acoustic oscillations and the local Hubble constant,” [Mon. Not. Roy. Astron. Soc. \*\*416\*\* \(Oct., 2011\) 3017–3032](#), [arXiv:1106.3366](#).
- [42] A. J. Ross, L. Samushia, C. Howlett, W. J. Percival, A. Burden, and M. Manera, “The clustering of the SDSS DR7 main Galaxy sample - I. A 4 per cent distance measure at  $z = 0.15$ ,” [Mon. Not. Roy. Astron. Soc. \*\*449\*\* \(May, 2015\) 835–847](#), [arXiv:1409.3242](#).
- [43] J. E. e. a. Bautista, “Measurement of baryon acoustic oscillation correlations at  $z = 2.3$  with SDSS DR12 Ly $\alpha$ -Forests,” [A&A \*\*603\*\* \(June, 2017\) A12](#), [arXiv:1702.00176](#).
- [44] H. e. a. du Mas des Bourboux, “Baryon acoustic oscillations from the complete SDSS-III Ly $\alpha$ -quasar cross-correlation function at  $z = 2.4$ ,” [ArXiv e-prints \(Aug., 2017\)](#), [arXiv:1708.02225](#).
- [45] E. A. Kazin, J. Koda, C. Blake, N. Padmanabhan, S. Brough, M. Colless, C. Contreras, W. Couch, S. Croom, D. J. Croton, T. M. Davis, M. J. Drinkwater, K. Forster, D. Gilbank, M. Gladders,

- K. Glazebrook, B. Jelliffe, R. J. Jurek, I.-h. Li, B. Madore, D. C. Martin, K. Pimbblet, G. B. Poole, M. Pracy, R. Sharp, E. Wisnioski, D. Woods, T. K. Wyder, and H. K. C. Yee, “The WiggleZ Dark Energy Survey: improved distance measurements to  $z = 1$  with reconstruction of the baryonic acoustic feature,” *Mon. Not. Roy. Astron. Soc.* **441** (July, 2014) 3524–3542, [arXiv:1401.0358](#).
- [46] M. e. a. Ata, “The clustering of the SDSS-IV extended Baryon Oscillation Spectroscopic Survey DR14 quasar sample: First measurement of Baryon Acoustic Oscillations between redshift 0.8 and 2.2,” *ArXiv e-prints* (May, 2017) , [arXiv:1705.06373](#).
- [47] F. Beutler, C. Blake, J. Koda, F. A. Marín, H.-J. Seo, A. J. Cuesta, and D. P. Schneider, “The BOSS-WiggleZ overlap region - I. Baryon acoustic oscillations,” *Mon. Not. Roy. Astron. Soc.* **455** (Jan., 2016) 3230–3248, [arXiv:1506.03900](#).
- [48] A. J. Cuesta, M. Vargas-Magaña, F. Beutler, A. S. Bolton, J. R. Brownstein, D. J. Eisenstein, H. Gil-Marín, S. Ho, C. K. McBride, C. Maraston, N. Padmanabhan, W. J. Percival, B. A. Reid, A. J. Ross, N. P. Ross, A. G. Sánchez, D. J. Schlegel, D. P. Schneider, D. Thomas, J. Tinker, R. Tojeiro, L. Verde, and M. White, “The clustering of galaxies in the SDSS-III Baryon Oscillation Spectroscopic Survey: baryon acoustic oscillations in the correlation function of LOWZ and CMASS galaxies in Data Release 12,” *Mon. Not. Roy. Astron. Soc.* **457** (Apr., 2016) 1770–1785, [arXiv:1509.06371](#).
- [49] V. Bonvin and et al., “H0LiCOW V. New COSMOGRAIL time delays of HE0435-1223:  $H_0$  to 3.8% precision from strong lensing in a flat  $\Lambda$ CDM model,” [arXiv:1607.01790v1](#).
- [50] R. Jimenez and A. Loeb, “Constraining Cosmological Parameters Based on Relative Galaxy Ages,” *Astrophys. J.* **573** (July, 2002) 37–42, [astro-ph/0106145](#).
- [51] M. Moresco, L. Pozzetti, A. Cimatti, R. Jimenez, C. Maraston, L. Verde, D. Thomas, A. Citro, R. Tojeiro, and D. Wilkinson, “A 6% measurement of the Hubble parameter at  $z \sim 0.45$ : direct evidence of the epoch of cosmic re-acceleration,” *JCAP* **5** (May, 2016) 014, [arXiv:1601.01701](#).
- [52] J. Lesgourgues, “The Cosmic Linear Anisotropy Solving System (CLASS) I: Overview,” [arXiv:1104.2932 \[astro-ph.IM\]](#).
- [53] D. Blas, J. Lesgourgues, and T. Tram, “The Cosmic Linear Anisotropy Solving System (CLASS) II: Approximation schemes,” *JCAP* **1107** (2011) 034, [arXiv:1104.2933 \[astro-ph.CO\]](#).
- [54] DES Collaboration, T. M. C. Abbott, et al., “Dark Energy Survey Year 1 Results: A Precise  $H_0$  Measurement from DES Y1, BAO, and D/H Data,” *ArXiv e-prints* (Nov., 2017) , [arXiv:1711.00403](#).
- [55] J. W. Henning et al., “Measurements of the Temperature and E-Mode Polarization of the CMB from 500 Square Degrees of SPTpol Data,” *ArXiv e-prints* (July, 2017) , [arXiv:1707.09353](#).
- [56] H. Lee, V. L. Kashyap, D. A. van Dyk, A. Connors, J. J. Drake, R. Izem, X.-L. Meng, S. Min, T. Park, P. Ratzlaff, A. Siemiginowska, and A. Zezas, “Accounting for Calibration Uncertainties in X-ray Analysis: Effective Areas in Spectral Fitting,” *ApJ* **731** (Apr., 2011) 126, [arXiv:1102.4610 \[astro-ph.IM\]](#).